Intermodulation Distortion in Kahn-Technique Transmitters

Frederick H. Raab, *Senior Member, IEEE*

Abstract— **The Kahn Envelope Elimination and Restoration (EER) technique implements a linear RF power amplifier (PA) by combining nonlinear, but efficient, RF and AF power amplifiers. For signals with high peak-to-average ratios, the average efficiency of a Kahn-technique transmitter can be three to four times that of a transmitter that employs conventional linear RF PA's. Since switching-mode amplifiers are employed, the linearity of an EER transmitter depends upon parameters such as the bandwidth of the envelope modulator and the differential delay between envelope and phase signals. This paper determines the relationship between these parameters and IMD levels and verifies the predictions by laboratory measurements. The results can be used to determine the requirements for the components of a Kahn-technique transmitter.**

I. Introduction

THE KAHN Envelope Elimination and Restoration (EER) technique [1] implements a linear RF power amplifier (PA) by combining RF and AF power amplifiers. In the classical form (Fig. 1), a limiter *eliminates* the envelope, producing a constant-amplitude, phase-modulated carrier. The detected envelope is amplified by the AF PA's. Amplitude modulation of the final RF PA *restores* the envelope to the phase-modulated carrier, creating an amplified replica of the input signal. In a modern implementation, the envelope and phase-modulated carrier are produced by a combination of digital signal processing and synthesis.

Nonlinear RF power amplifiers (e.g., classes C, D, E, and F) offer better efficiency than do linear PA's (classes A and B) [2], [3]. High-efficiency high-level amplitude modulation is accomplished by class-S or -G AF PA's. While conventional linear transmitters suffer from poor efficiency for low-amplitude signals, Kahn-technique transmitters have good efficiency over a wide dynamic range.

The efficiency of conventional transmitters that use class-A or -B PA's can be rather poor for typical voice-modulated, noise, and multitone signals with large peak-to-average ratios. For example, ideal class-A and -B PA's have average efficiencies of only 5 and 28%, respectively, when amplifying a Rayleigh-envelope noise with a 10-dB peak-to-average ratio [4]. As a result, a Kahn-technique transmitter can be several times as efficient as conventional transmitters [5].

The Kahn technique is currently being used in a number of applications where efficiency is critical. A medium-power HF transmitter employs a class-D RF PA and a class-S modulator and achieves an efficiency of about 60% for virtually all signals [6]. A low-power UHF transmitter employs a class-E RF PA and a class-S modulator and also achieves an overall efficiency of 60% over most of its dynamic range [7]. A high-power SSB broadcast transmitter employs class-C RF PA's and pulse-step amplitude modulators [8]. Hardman describes a medium-power satellite transponder [9] and Bateman notes its use for ACSSB at 220 MHz [10].

The linearity of a Kahn transmitter does not depend upon the linearity of its RF-power transistors. Processes such as pulse-width modulation also do not depend upon the linearity of individual transistors. Consequently, the intermodulation-distortion (IMD) characteristics of an EER transmitter depend primarily upon parameters such as the bandwidth of the envelope modulator and the difference in the delay between the envelope and phase signals when they are recombined in the final amplifier.

The IMD characteristics of EER are mentioned only briefly in the original paper by Kahn [1]. More recently, simulation results [11], [12] have provided relevant information. This paper derives the IMD relationships for the for the two principal system limitations:

1) finite envelope bandwidth;
2) differential delay between envelope and carrier.

The theoretical predictions are based upon the commonly used two-tone test signal and are validated by laboratory measurements. The results can be used by transmitter designers to determine the parameters required for a Kahn transmitter to achieve a specified IMD performance.

Intermodulation distortion is, of course, also produced by hardware imperfections such as nonlinear transfer functions and amplitude-to-phase conversion. Several techniques have been developed to improve the linearity due to such causes. These include envelope feedback [13], polar loop (envelope feedback and phase lock) [14], and Cartesian feedback (feedback of I and Q components) [15], and predistortion [16].

II. Experimental Transmitter

The block diagram of the experimental EER transmitter [5], [6] is shown in Fig. 1. Its principal components are an SSB modulator, delay network, frequency converter, class-S modulator, and class-D RF power amplifier.

Signals are generated by a conventional filter-type SSB modulator. A variable dc bias allows either full-carrier AM or carrier nulling for SSB/SC. Operation at 10.7 MHz allows

Manuscript received March 25, 1996; revised August 26, 1996.

The author is with the Green Mountain Radio Research Laboratory, Colchester, VT 05446 USA.

Publisher Item Identifier S 0018-9480(96)08510-9.

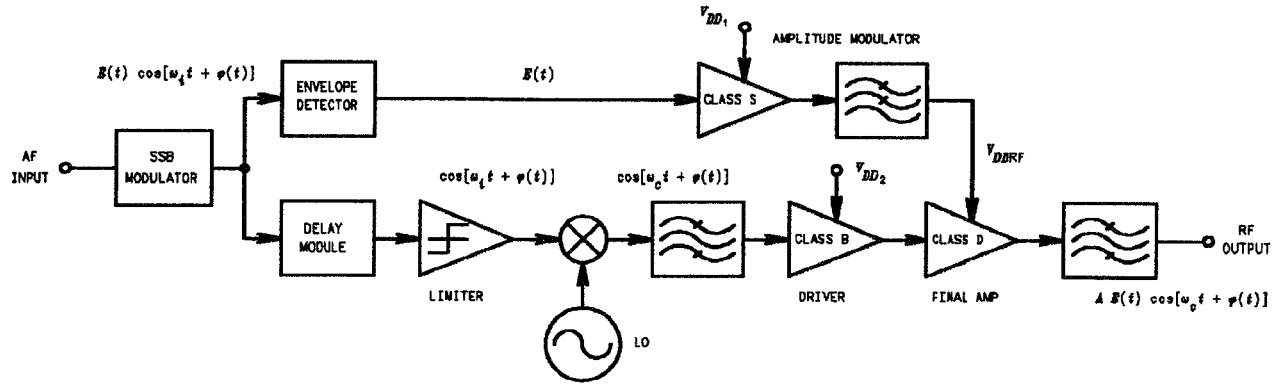

Fig. 1. Block diagram of experimental Kahn-technique transmitter.

for highly linear synchronous envelope detection as well as limiting with low amplitude-to-phase conversion.

Delaying the hard-limited 10.7-MHz IF signal is accomplished by down-conversion to baseband (I and Q) components, delaying the baseband components, up-conversion to 10.7 MHz, and recombination to form the delayed RF signal. Delay of the I and Q components is accomplished by a chain of op-amp all-pass filters followed by a tapped delay line. This combination allows delays up to 20 μs in 100-ns steps.

The hard-limited signal is translated to the desired output frequency by a double-conversion scheme (shown for simplicity in Fig. 1 as single conversion). The first conversion by a fixed LO translates the signal to an IF well above the output pass band. The second conversion by the VFO translates the high-IF signal down to the output frequency.

The class-S modulator used in the EER transmitter [17], [18] has a switching frequency of about 250 kHz, an envelope bandwidth of 57 kHz, a power output of 150 W, an efficiency of about 90%, and a linearity of about 1%. The four-pole Butterworth output filter introduces a delay of about 9 μs.

The class-D RF-power amplifier [19] is based upon a pair of MRF148 MOSFET's in a transformer-coupled voltage-switching configuration. Broadband Guanella (equal-delay) transformers are used at both the input and output. The PA produces an output of 80 to 100 W and operates from 1 to 60 MHz. The efficiency is on the order of 75–78% at frequencies up to 20 MHz and then drops toward about 50% at 60 MHz. It is essentially constant for all signal amplitudes. The amplitude-modulation linearity (supply voltage to RF-output voltage) curve differs from a straight line by 1.24% rms.

III. Two-Tone Test Signal

The relative simplicity of the commonly used two-tone (two-carrier) test signal allows the derivation of analytic relationships between each of the system parameters and the IMD. This section derives the basic formulations to be used subsequently. The waveforms are shown in Fig. 2.

The input and output signals are described by

$$\begin{aligned} v_i(t) &= \tfrac{1}{2}[\cos(\omega_c\omega_m)t + \cos(\omega_c - \omega_m)t] \\ &= E_i(\theta)\cos[\omega_c t + \phi_i(\theta)] \end{aligned} \tag{1}$$

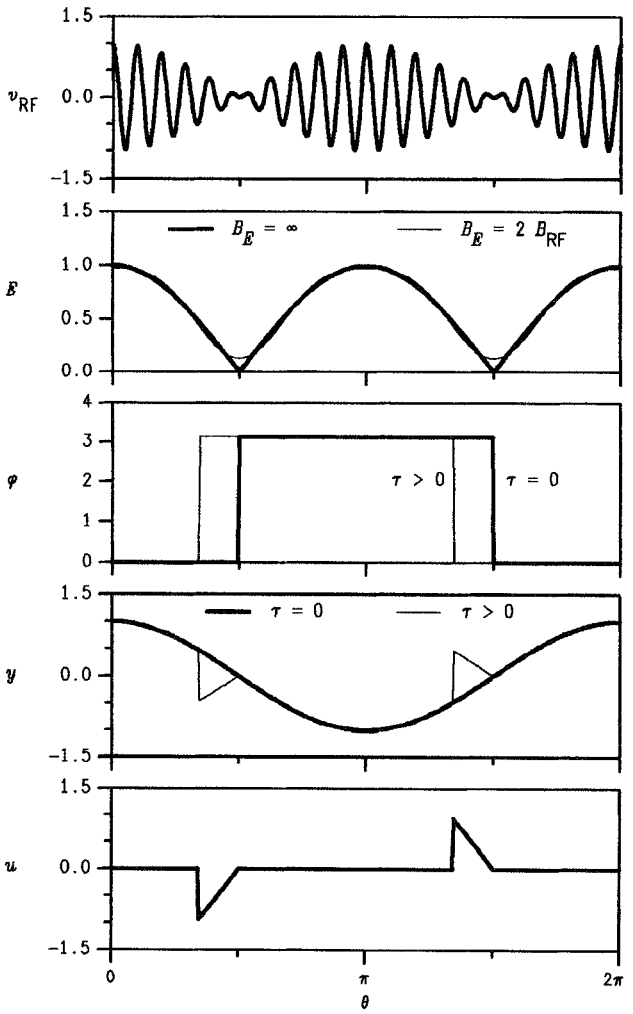

Fig. 2. Waveforms in Kahn-technique transmitter.

and

$$v_0(t) = E_0(\theta - \tau)\cos[\omega_c t + \phi_0(\theta)] \tag{2}$$

where $\theta = \omega_m t$ and τ is the envelope-phase delay in radians. The bandwidth of the RF signal is

$$B_{\mathrm{RF}} = 2\omega_m. \tag{3}$$

The envelope and phase functions for the two-tone test signal are

$$E_i(\theta) = |\cos\theta| \tag{4}$$

and

$$\phi_i(\theta) = \frac{\pi}{2}[1 - c(\theta)] \tag{5}$$

respectively, where $c(\theta)$ is a square wave with amplitudes of $+1$ or -1 and cosinusoidal phasing.

Expansion of the envelope function as a Fourier series produces

$$E_0(\theta) = [a_0 + \sum_{m=2,4,6,\cdots} a_m \cos m\theta] \tag{6}$$

where

$$a_m = \begin{cases} \frac{2}{\pi}, & m = 0 \\ \frac{4}{\pi}\frac{(-1)^{(m-2)/2}}{(m^2-1)}, & m \geq 2. \end{cases} \tag{7}$$

A similar expansion of the switching function yields

$$c(\theta) = \sum_{n=1,3,5,\cdots} c_n \cos n\theta \tag{8}$$

where

$$c_n = \frac{4}{\pi}\frac{(-1)^{(n-1)/2}}{n}. \tag{9}$$

IV. Effects of Envelope Bandwidth

The bandwidth of the class-S modulator sets the bandwidth B_E of the high-power envelope signal. The bandwidth of the modulator is determined by design compromises involving linearity, efficiency, and spurious products. Envelope bandwidths from 5 to 100 kHz are typical.

A. Theory

For a two-tone signal, the phase changes are equivalent to reversals in the carrier polarity. Consequently, the effects of finite envelope bandwidth can be determined by moving the switching function $c(\theta)$ outside of the cosine function in (2) and then combining it with the envelope function, thus

$$v_0(t) = E_0(\theta)c(\theta)\cos\omega_c t = y(\theta)\cos\omega_c t. \tag{10}$$

If the output envelope is an exact replica of the input envelope, then $y(\theta) = \cos\theta$.

The modulation function $y(\theta)$ can be represented as the Fourier series

$$y(\theta) = b_1\cos\theta + b_3\cos 3\theta + b_5\cos 5\theta + \cdots. \tag{11}$$

The coefficient b_1 corresponds to the amplitude of the desired sidebands; the higher-order coefficients $(b_3, b_5, \cdots)$ correspond to the amplitudes of the IMD products.

The effect of an abrupt-junction filter in the envelope channel is modeled by truncating the Fourier series (5) after the Mth component, thus

$$E_0(\theta) = [a_0 + \sum_{m=2,4,\cdots,M} a_m \cos m\theta]. \tag{12}$$

TABLE I
C/I as a Function of Envelope Bandwidth from Theory

B_E/B_{RF}	C/I_{max},
0	17.39
1	31.37
2	37.53
3	41.87
4	45.23
5	47.98
6	50.31
7	52.33
8	54.12
9	55.72
10	57.17
11	58.49
12	59.71
13	60.85
14	61.90
15	62.89

Since the RF bandwidth (3) of the two-tone signal is $2\omega_m$

$$M = \text{int}\left(\frac{2B_E}{B_{RF}}\right) \tag{13}$$

where "int" represents rounding to the nearest smaller integer.

The spectral components of modulation function $y(\theta)$ are produced by mixing each of the spectral components of $E_0(\theta)$ with each of the spectral components of $c(\theta)$. Since

$$2\cos n\theta\cos m\theta = \cos(m+n)\theta + \cos(m-n)\theta \tag{14}$$

the coefficients b_k in (11) have the forms

$$b_1 = \tfrac{1}{2}[2a_0c_1 + a_2(c_1 + c_3) + a_4(c_3 + c_5) + \cdots] \tag{15}$$

$$b_3 = \tfrac{1}{2}[2a_0c_3 + a_2(c_1 + c_5) + a_4(c_3 + c_7) + \cdots] \tag{16}$$

$$b_5 = \tfrac{1}{2}[2a_0c_5 + a_2(c_3 + c_7) + a_4(c_1 + c_9) + a_6(c_1 + c_{11}) + a_8(c_3 + c_{13}) + \cdots]. \tag{17}$$

etc.

The terms in (15)–(17) have the form $a_m(c_{|m-k|} + c_{m+k})$. Consequently, they eventually decrease as either $1/m^3$ or $1/m^4$, depending whether the two c_n are of the same or different sign. Determination of the values of the coefficients b_k is most readily accomplished numerically.

Since modulation of the carrier by $y(\theta)$ produces two components of amplitude $b_k/2$, the carrier-to-intermodulation ratio is

$$(C/I)_{dB} = 20\log(2/|b_k|). \tag{18}$$

This C/I ratio is defined with respect to an *unmodulated carrier* (amplitude of unity).

The resultant theoretical predictions of the C/I ratio are shown in Fig. 3 as a function of B_E/B_{RF}; corresponding values are given in Table I. The order of the maximum-amplitude IM product increases with B_E/B_{RF}, hence the third-order IM product is not generally the maximum IM product. For example, if $B_E = 4B_{RF}$, the ninth-order product is the largest. Simulations [11] show that the IMD for multitone signals is never larger than that of the two-tone signal. Obtaining C/I $\geq$ 30 dBc therefore requires $B_E \geq B_{RF}$, while C/I $\geq$ 40 dBc requires $B_E \geq 3B_{RF}$.

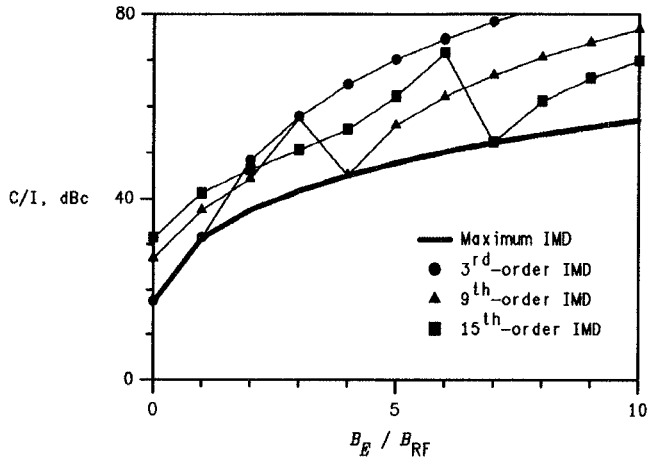

Fig. 3. IMD levels for finite envelope bandwidth (theory).

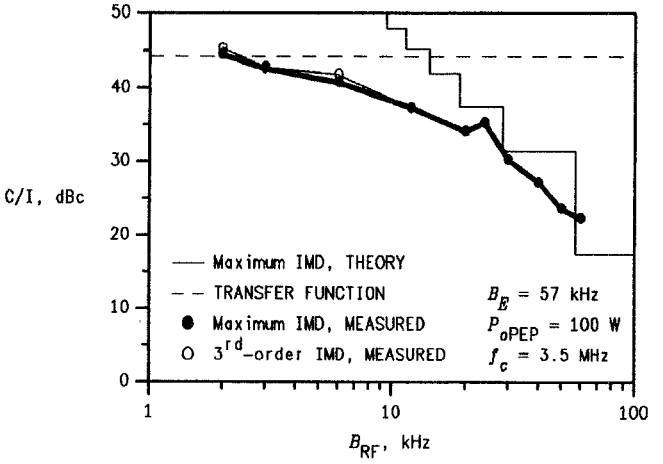

Fig. 4. Variation of IMD level with envelope bandwidth (measured).

B. Measurements

The variation of the measured C/I_{max} with B_{RF} for $B_E = 57$ kHz and the best delay match is shown in Fig. 4. The stair-step function represents the worst-case C/I level predicted by theory. The dashed line represents the 1.24% rms dc-linearity error (rms deviation of the transfer function from a straight line) of the combined RF PA and modulator. For RF signals of small bandwidths, the transfer-function errors dominate. For larger bandwidths, the effects of the bandwidth of the envelope modulator dominate and the observed IM levels transition to those predicted by theory.

In the laboratory measurements, the third-order product is almost always the worst IM product. Peaking of higher-order IM products at certain values of B_E/B_{RF} is not observed. Instead, it appears that the first three odd-order products are dominant and of somewhat equal amplitude (Fig. 5). The value of C/I decreases smoothly with B_E rather than in the stair-step manner predicted by theory.

The theory is based upon an abrupt-cutoff filter. In contrast, any real filter has a gradual roll-off characteristic (four-pole Butterworth in this case). The difference between the observed and predicted IM behavior is likely due to a combination of the gradual roll-off and the limits imposed by dc linearity.

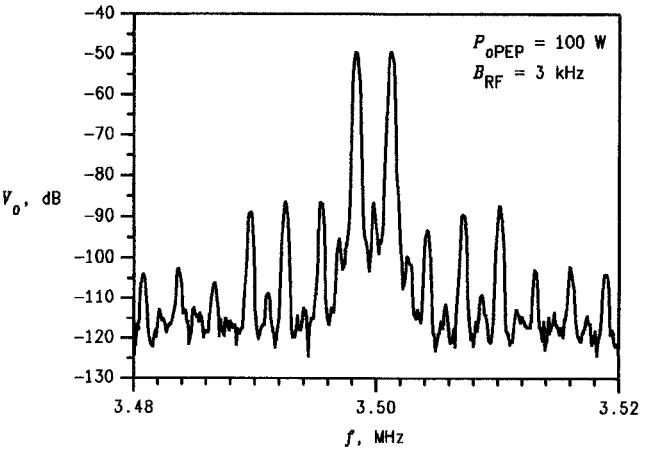

Fig. 5. Measured IMD spectrum for voice-bandwidth test signal.

The laboratory measurements also contain low-level even-order IM products that are not predicted by theory. These are thought to be due to imperfect suppression of the carrier in the SSB modulator.

V. Effects of Differential Delay

The class-S modulator employs a low-pass output filter to suppress the switching frequency and its harmonics. Generally, four to six poles are required. Delay is inherent in any filter and increases as bandwidth decreases. Typically, the envelope signal is delayed from 5 to 20 μs, while the carrier signal is delayed by only 1 to 2 μs. To minimize output IMD, the modulator and signal-processing circuitry must add delay to the phase-modulated carrier to equalize the two delays. Errors in equalizing the two delays result in an imperfectly reconstructed RF signal, hence IMD.

A. Theory

The effects of differential delay can be analyzed by shifting the alignment of the envelope and phase-switching functions as shown in Fig. 1. The effect of mismatched envelope and phase waveforms is to invert the polarity of the (DSB/SC) amplitude-modulation function $y(\theta)$ during two parts of the cycle. The resultant IMD is then equivalent to an additive function $u(r)$.

For convenience in analysis, it is preferable to advance the phase-switching waveform rather than to retard the envelope. The equivalent amplitude-modulation function for the output signal is therefore

$$y(\theta) = |\cos\theta| c(\theta + \tau) = \cos\theta + u(\theta) \tag{19}$$

where

$$u(\theta) = \begin{cases} -2\cos\theta, & \pi/2 - \tau \le \theta < \pi/2 \\ -2\cos\theta, & 3\pi/2 - \tau \le \theta < 3\pi/2 \\ 0, & \text{otherwise.} \end{cases} \tag{20}$$

The differential delay τ in radians is related to the differential delay in seconds (Δt) by

$$\Delta t = \frac{\tau}{2\pi}\frac{1}{f_m} = \frac{\tau}{2\pi}\frac{2}{B_{RF}} = \frac{\tau}{\pi B_{RF}}. \tag{21}$$

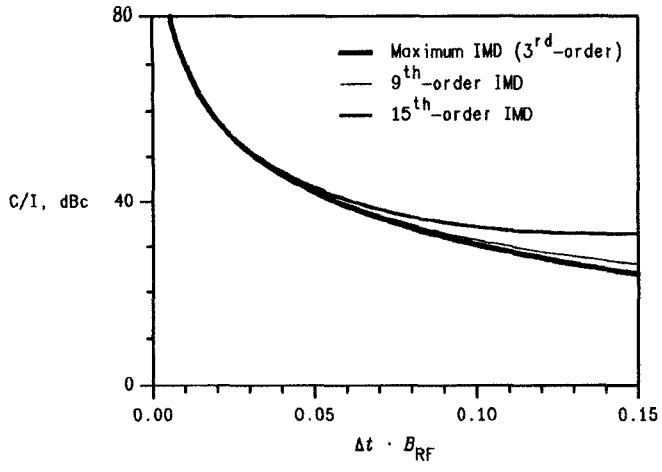

Fig. 6. IMD levels for nonzero differential delay (theory).

Since only the magnitude of the IMD products is of interest, it is more convenient to analyze

$$u'(\theta) = \begin{cases} -2\sin\theta, & 0 \le \theta < \tau \\ -2\sin\theta, & \pi \le \theta < \pi + \tau \\ 0, & \text{otherwise.} \end{cases} \tag{22}$$

To determine the IMD products, $u'(\theta)$ is expanded into the Fourier series

$$u'(\theta) = \sum_{k=1}^{\infty} (a_k \cos k\theta + b_k \sin k\theta). \tag{23}$$

(This a_k and b_k are *not* the same a_k and b_k used in the previous section.)

Symmetry dictates that the even-order coefficients are zero. The odd-order coefficients are

$$a_k = (-4/\pi) \int_0^{\tau} \sin\theta \cos k\theta \, d\theta \tag{24}$$

$$= (-2/\pi) \left[\frac{1 - \cos(k+1)\tau}{k+1} + \frac{\cos(k-1)\tau - 1}{k-1} \right]. \tag{25}$$

For $|z| \ll 1, \cos z \approx 1 - z^2/2$. Therefore, for $k\tau \ll 1$

$$a_k \cong (-2/\pi) \left[\frac{(k+1)^2\tau^2/2}{(k+1)} - \frac{(k-1)^2\tau^2 2}{k-1} \right]$$

$$= (-2/\pi)\tau^2. \tag{26}$$

Similarly

$$b_k = (-4/\pi) \int_0^{\tau} \sin\theta \sin k\theta \, d\theta \tag{27}$$

$$= (-2/\pi) \left[\frac{\sin(k-1)\tau}{k-1} - \frac{\sin(k+1)\tau}{k+1} \right]. \tag{28}$$

For $k\tau \ll 1$

$$b_k \cong (-2/\pi) \left[\frac{(k-1)\tau}{k-1} - \frac{(k+1)\tau}{k+1} \right] \approx 0. \tag{29}$$

For small delays, the magnitude of the IM product is therefore approximately

$$c_k = (a_k^2 + b_k^2)^{1/2} \approx |a_k| = (2/\pi)\tau^2. \tag{30}$$

TABLE II
C/I AS A FUNCTION OF DIFFERENTIAL DELAY FROM THEORY

$\Delta t \cdot B_{\mathrm{RF}}$	$\mathrm{C/I_{max}}$,
0.010	70.06
0.015	63.02
0.020	58.03
0.025	54.16
0.030	51.00
0.035	48.33
0.040	46.02
0.045	43.99
0.050	42.17
0.060	39.03
0.070	36.39
0.080	34.12
0.090	32.12
0.100	30.34
0.110	28.75
0.120	27.30
0.130	25.98
0.140	24.78
0.150	23.66
0.200	19.17
0.225	17.44
0.250	15.96

The theoretical prediction of C/I as a function of delay is shown in Fig. 6 with corresponding values in Table II. Obtaining C/I $\geq$30 dBc requires $\Delta t \leq 0.1/B_{\mathrm{RF}}$, while C/I $\geq$40 dBc requires $\Delta t \leq 0.057/B_{\mathrm{RF}}$. For speech-bandwidth signals ($B_{\mathrm{RF}} = 3$ kHz), 30- and 40-dBc C/I requirements imply differential delays of no more than 34 and 19 μs, respectively. The IMD spectrum consists of odd-order products whose amplitudes decrease slowly with increasing order. Simulations [11] show that the IMD for multicarrier signals is generally lower than that for a two-tone signal.

B. Measurement

An RF bandwidth of 20 kHz produces good sensitivity of IMD levels to changes in delay while keeping the delay-related IMD's below those due to finite envelope bandwidth and dc nonlinearity. Measured IM spectra produced by near-optimum and 6-μs differential delays are shown in Fig. 7. The odd-order IM products dominate. While the roll-off is not flat [as predicted by the approximation in (30)], it is slow. The differences between upper and lower sidebands are probably due to constructive and destructive combinations of IM products from different sources.

The variation of $\mathrm{C/I_{max}}$ with the delay added to the carrier (phase modulation) is shown in Fig. 8. The best C/I is obtained with $t_D \approx 7$ μs, as expected. The maximum C/I is limited by both dc nonlinearities and the finite envelope bandwidth. However, the theoretical predictions match the measurements closely when the differential delay is sufficiently large to allow the delay-related IMD to be clearly dominant. In this region, the predicted change of 6 dB with doubling of the delay is readily observed.

VI. CONCLUSIONS AND RECOMMENDATIONS

The measurements presented here generally verify the theoretical predictions for the IMD produced by finite envelope

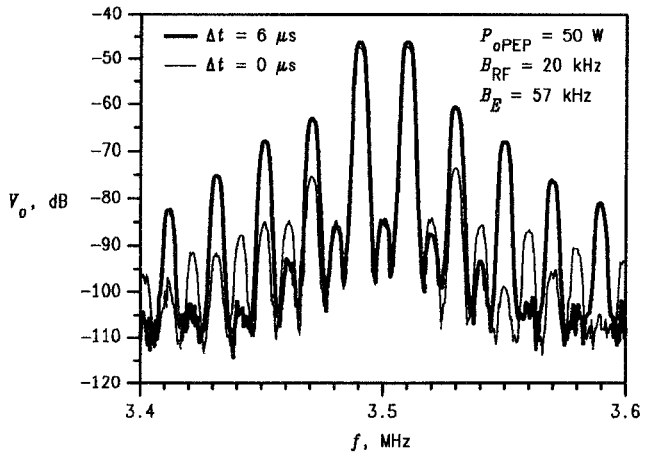

Fig. 7. IMD spectrum produced by nonzero differential delay.

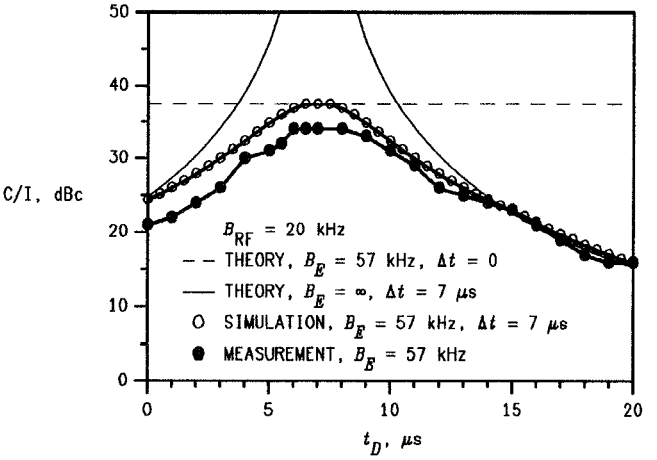

Fig. 8. Variation of C/I with differential delay (measured).

bandwidth and nonzero differential delay in a Kahn-technique transmitter. The errors between theory and measurement are within the limits of the known measurement errors. The theory can therefore be used with confidence to determine the requirements for EER transmitters.

Discrepancies in the roll-off of the IM products and the presence of several low-level products of unknown origin suggest further investigations in the following areas:

1) effects of real (nonabrupt) envelope filters;
2) IMD levels for tones with unequal amplitudes;
3) IMD due to finite carrier bandwidth;
4) spurious products inherent in PWM.

ACKNOWLEDGMENT

The Kahn-technique transmitter was built under Contract DAAB10-86-C-0585 from the U.S. Army CECOM Integrated Electronic Warfare Directorate at Vint Hill, VA. The IMD data were collected as part of a GMRR IR&D effort. D. J. Rupp assisted in collection of the data.

REFERENCES

[1] L. R. Kahn, "Single sideband transmission by envelope elimination and restoration," *Proc. IRE*, vol. 40, no. 7, pp. 803–806, July 1952.
[2] H. L. Krauss, C. W. Bostian, and F. H. Raab, *Solid State Radio Engineering*. New York: Wiley, 1980.
[3] F. H. Raab, *High-Efficiency Power Amplifiers* (Seminar Notebook). Colchester, VT: Green Mountain Radio Research, 1989.
[4] ——, "Average efficiency of power amplifiers," in *Proc. RF Technology Expo '86*, Anaheim, CA, Jan. 30–Feb. 1, 1986, pp. 374–486.
[5] F. H. Raab and D. J. Rupp, "High-efficiency single-sideband HF/VHF transmitter based upon envelope elimination and restoration," in *Proc. Sixth Int. Conf. HF Radio Systems and Techniques (HF'94)*, York, U.K., July 4–7, 1994, pp. 21–25.
[6] F. H. Raab and D. J. Rupp, "High-efficiency multimode HF/VHF transmitter for communication and jamming," in *Proc. MILCOM'94*, Ft. Monmouth, NJ, Oct. 2–5, 1994, pp. 880–884.
[7] T. Sowlati, Y. Greshishchev, C. Andre, T. Salama, G. Rabjohn, J. Sitch, "Linear transmitter design using high efficiency class E power amplifier," in *Proc. Int. Symp. Personal, Indoor, and Mobile Radio Commun.*, Toronto, Sept. 1995, pp. 1233–1237.
[8] B. Weaver, "A new, high efficiency, digital, modulation technique for AM or SSB sound broadcasting appliciations," in *Proc. Int. Symp. Broadcasting Technol.*, Zhuhai, 1991.
[9] G. E. Hardman, "A linear transponder for a mobile satellite system," in *Proc. IEE Conf. Mobile Radio Systems and Techniques*, Sept. 1984, pp. 216–219.
[10] A. Bateman, P. Kennington, J. P. McGeehan, and M. Beach, "Multimode transceiver design," in *Proc. RF Expo West '94*, San Jose, CA, Mar. 22–24, 1994, pp. 327–331.
[11] F. H. Raab, "Envelope-elimination-and-restoration system requirements," in *Proc. RF Technology Expo '88*, Anaheim, CA, Feb. 10–12, 1988, pp. 499–512.
[12] K. Meinzer, "A linear transponder for amateur radio satellites," *VHF Commun.*, vol. 7, pp. 43–57, Jan. 1975.
[13] W. B. Bruene, "Distortion reducing means for single-sidedband transmitters," *Proc. IRE*, vol. 44, no. 12, Dec. 1956, pp. 1760–1765.
[14] V. Petrovic and W. Gosling, "Polar-loop transmitter," *Electron. Lett.*, vol. 15, no. 10, pp. 286–287, May 10, 1979.
[15] V. Petrovic and A. N. Brown, "Application of Cartesian feedback to HF SSB transmitters," in *Proc. Third Int. Conf. HF Commun. Systems and Techniques*, Feb. 26–28, 1985, pp. 81–85.
[16] J. Cavers, "Amplifier linearization using a digital predistorter with fast adaptation and low memory requirements," *IEEE Trans. Veh. Technol.*, vol. 39, no. 4, pp. 374–382, Nov. 1990.
[17] F. H. Raab and D. J. Rupp, "Class-S high-efficiency amplitude modulator," *RF Design*, vol. 17, no. 5, pp. 70–74, May 1994.
[18] ——, "High-efficiency amplitude modulator," in *Proc. RF Expo East '94*, Orlando, FL, Nov. 15–17, 1994, pp. 1–9.
[19] ——, "HF power amplifier operates in both class B and class D," in *Proc. RF Expo West '93*, San Jose, CA, Mar. 17–19, 1993, pp. 114–124.

Frederick H. Raab (S'66–M'72–SM'80) received the B.S., M.S., and Ph.D. degrees in electrical engineering from Iowa State University, Ames, in 1968, 1970, and 1972, respectively.

He is Chief Engineer and Owner of GMRR, which he founded in 1980. He is coauthor of *Solid State Radio Engineering* (New York: Wiley, 1980) and over 70 technical papers, and he holds four patents. His professional activities include RF power amplifiers and transmitters, low-frequency and through-the-earth communication systems, and the magnetic helmet-mounted sight.

Dr. Raab is a member of HKN, Sigma Xi, AOC, and AFCEA. He is extra-class amateur-radio operator WA1WLW, licensed since 1961. He was Program Chairman of RF Expo East '90 and received Iowa State University's Professional Achievement Citation in Engineering in 1995.